4-2014

Development of a Spring-Based Automotive Starter

David H. Myszka
University of Dayton, dmyszka1@udayton.edu

Jonathan Lauden
University of Dayton

Patrick Joyce
University of Dayton

Andrew P. Murray
University of Dayton, amurray1@udayton.edu

Christoph Gillum
Stress Engineering Services

2014-01-1932
Published 04/01/2014

doi:10.4271/2014-01-1932
saecomveh.saejournals.org

Development of a Spring-Based Automotive Starter

David H. Myszka, Jonathan Lauden, Patrick Joyce, and Andrew Murray
University of Dayton

Christoph Gillum
Stress Engineering Services Inc.

ABSTRACT

Automotive starting systems require substantial amounts of mechanical energy in a short period of time. Lead-acid batteries have historically provided that energy through a starter motor. Springs have been identified as an alternative energy storage medium and are well suited to engine-starting applications due to their ability to rapidly deliver substantial mechanical power and their long service life. This paper presents the development of a conceptual, spring-based starter. The focus of the study was to determine whether a spring of acceptable size could provide the required torque and rotational speed to start an automotive engine. Engine testing was performed on a representative 600 cc, inline 4-cylinder internal combustion engine to determine the required torque and engine speed during the starting cycle. An optimization was performed to identify an appropriate spring design, minimizing its size. Results predict that the test engine could be started by a torsional steel spring with a diameter and length of approximately 150 mm, similar in size, but lower weight than an electrical starting system of the engine. A proof-of-concept prototype has been constructed and evaluated.

CITATION: Myszka, D., Lauden, J., Joyce, P., Murray, A. et al., "Development of a Spring-Based Automotive Starter," *SAE Int. J. Commer. Veh.* 7(1):2014, doi:10.4271/2014-01-1932.

1. INTRODUCTION

An increasing concern for sustainability has lead to dramatic growth of electric and hybrid-vehicles. Still, the internal combustion (IC) engine is the dominant propulsion device for automotive and commercial vechicles [1]. An increased focus on improving the fuel efficiency in these traditonal vehicles fostered recent developments including the use of alternative fuels [2], reduced friction within engines [3] and efficient continuously variable transmissions [4]. Turning the engine off during idle stops will increase fuel efficiency and is widely employed in hybrids.

An IC engine is not a self-starting device as the pistons must be moving to draw in the fuel-air mixture into a cylinder and be compressed prior to combustion [5]. Thus, starting requires initial engine cranking by an auxiliary source. The minimum rotational speed required to start a typical IC engine is approximately 100 to 200 rpm [6]. However, the crankshaft torque depends on the engine type, swept volume and number of cylinders. The earliest automobile engines were started with hand cranks, where the driver was capable of providing the necessary speed and torque. This proved to be difficult and dangerous for the operator, as the engine could backfire and cause injury to the hand crank operator [7]. To address this issue, Charles Kettering patented the electric self-starter in 1915 [8]. The fundamental concept has changed little to this day and is comprised of a battery-driven DC motor, pinion engaging transmission and a device that disengages the strater from the drive shaft once the engine is started. Since the speed of a DC motor is significantly higher than the engine requirements, the starter transmission (starter pinion and engine ring gear) has a suitable step-down ratio (approximately 1:10 to 1:20).

A starter battery stores chemical energy, which must rapidly be converted into electrical energy and supply a high current in order to start the engine. Having an energy density of approximately 140 kJ/kg [9], lead-acid storage batteries are most often used. However, the large size of the battery and large diameter copper cables are direclty attributed to the need for rapid extraction of energy required by the starter. That is, the moderate power density of batteries is a fundamental design challenge. To that end, idle-stop systems are less frequently used with IC engines than hybrids, as they require an upgraded starter/generator and battery [10]. Additionally, a control system is used to monitor auxiliary loads and depth of battery discharge as protection from advanced aging. An additional drawback of large batteries is the environmental concerns that exist with manufacture and disposal of batteries [11].

Elastic energy storage has been used for hundreds of years for applications such as bows, tweezers and clocks. At approximately 0.3 kJ/kg [12], the specific energy density of a steel spring is much less than batteries and not commonly considered as a viable option for wide-spread, high energy storage. Yet despite having a low energy density, springs are able to rapidly release their stored energy. This large power density can make a spring attractive for engine starting applications. The storage attractiveness is improved when using hyperelastic springs, such as rubber with an energy density of 12 kJ/kg [12], but can raise durability concerns. Current research involves constructing springs from carbon nano-tubes (CNT), having an energy density of 800 kJ/kg and vastly exceeding the capacity of batteries [13]. Commercialization of CNT technology greatly enhances the attractiveness of a spring starting system.

Spring starters have been commerically available on small lawn mowers [14], and large remote power generators [15]. When compared to a large battery and high amperage starter motor, it is anticipated that a spring starter could have lower weight, longer life and no disposal concerns. In order to evaluate the feasibility of using an elastic storage member for the engine-starting system, this paper presents a study that determines the size of a steel torsional spring to start an four-cylinder, IC engine. The remainder of the paper is organized as follows. Section 2 introduces the conceptual model of a spring starter. Section 3 describes the representative test engine. Section 4 presents experiments used to characterize the starter motor and engine. Section 5 describes an optimization performed to select an appropriate spring. Section 6 presents the proof-of-concept prototype and evaluation.

2. DESCRIPTION OF CONCEPT

The device being evaluated is not indended to eliminate the battery. Besides starting the engine, the battery in an automotibile is required for various ancillary devices. Instead, the spring starter system is expected to significantly reduce the size of the battery and associated cables.

A conceptual schematic of a spring-based mechanical starter is shown in Fig. 1. The primary feature of the system is the use of a spring rather than a battery to store energy. The spring can take many geometric forms. A spring formed through tensile bands most efficiently utilizes the material as the entire section is stressed at the same level. Springs that are formed through torsional or bending elements can use space more effectively and reduce hazard due to a potential failure [16]. Extension and torsional coil springs are widely used in general machine applications and have predictable behavior and reliability [17].

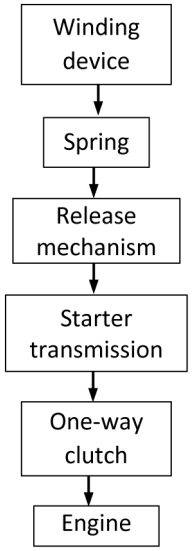

Figure 1. Conceptual model of a spring starter.

A sketch of the physical realization of the spring-based starter concept is shown in Fig. 2. One end of the spring is deflected by a worm gear drive, storing and locking energy in the spring. The other end of the spring is coupled to the engine shaft via transmission gears. A latching mechanism is placed between the spring and the transmission gears and is engaged when necessary to prevent the system from releasing energy. A one-way or overrunning clutch is mounted to the final gear of the transmission, such that the system is coupled to the engine during the starting cycle and decoupled during normal engine operation.

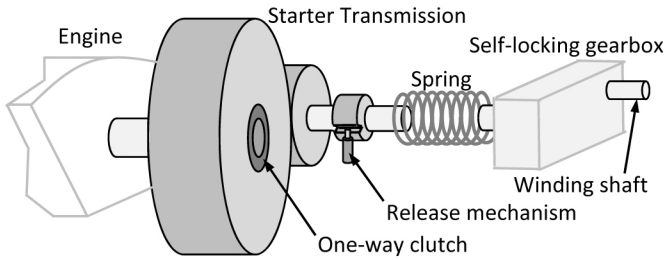

Figure 2. Physical realization of a spring starter concept.

The device is charged by rotating the input shaft to the worm gear drive while the latching mechanism is engaged. This wind can occur manually or from a novel device that is coupled to the running engine. Due to the large gear reduction within the worm gear, the spring can also be deformed by a small DC motor, powered by the alternator or small battery, which charges the spring over a longer period of time. Further evaluation of these options is left for future work.

The stored energy is discharged by releasing the latching mechanism, thus allowing the spring to exert torque on the transmission gears and transfering power to the engine. The transmission ratio can be chosen to provide a match of the torque and speed delivered by an optimal spring and the engine starting requirements.

Note that the concept described uses all the spring energy for a single crank cycle. A drawback is the inability to recrank in the case of misfire. In this case, the driver must wait for the small dc motor to energize spring or the spring must be deformed manually (taking advantage of the large ration in the self-locking gearbox). Further investigation into solutions for this drawback is also left for future work.

3. TEST PLATFORM

To evaluate the capability of a spring-starter system in a representative automotive application, a suitable test platform was obtained. A 1995 Yamaha XJ600S motorcycle engine was selected to serve as a platform for system development. A motorcycle was identified as having several desirable features, namely: it is easy to transport, relatively small, and has an accessible engine. The XJ600S is similar to the most common configuration of automobile engine, having an in-line four-cylinder, four-stroke IC engine equipped with an electric starter motor. The shared features suggest that if a well-sized spring starter system were to successfully crank the XJ600S engine, the design could be adapted to automotive engines. The specifications of the electric starting system on this engine provide a design goal for weight and size of the spring starter prototype.

The starting system of the Yamaha XJ600S is actuated by a Mitsuba SM-13 brushed DC motor, with a rated output of 0.8 kW [18]. According to these rating point specifications, the motor draws a peak current of 67 amps from a 12-volt lead-acid battery. The 151×106×87 mm. CBTX9-BS battery weighs 2.5 kg and is rated for 120 cold cranking amps and a capacity of 8 amp-hours.

Installed on the motorcycle, the starter motor transmits mechanical power to the crankshaft through a compound gear train. The shaft of the starter motor has 10 teeth cut into the end, and is in constant mesh with the starter clutch shaft via an idler gear. The starter clutch shaft is fitted with a one-way clutch, which in turn drives a chain that rotates the crankshaft. The starting clutch transmission provides a 27:1 gear ratio between the starter motor shaft and the crankshaft.

4. CHARACTERIZING THE TEST ENGINE

To develop a dynamic model of the engine and determine a set of design criteria, the torque, angular velocity, and duration of engine rotation provided by the electric starter system must be known. This information is not readily available and must be determined through experimental methods. This was accomplished in two steps: understand the relationship between torque and current in the starter motor and use that relationship to estimate the torque by measuring current. Once the torque constant of the motor is known, the current draw of the motor may be used to determine the torque developed during engine starting.

Starter Motor

A brushed DC motor exhibits a linear relationship between applied current I, start-up current I_0 and output torque T_s [19], represented by a torque constant k_t

$$T_s = k_t \left(I - I_0 \right). \tag{1}$$

An experimental method was used to characterize the starter motor by determining k_t and I_0. A Prony brake, as shown in Fig. 3, was used to measure the relationship between the amperage and torque for the starter motor. A Prony brake is a form of dynamometer and is an established method of motor performance testing [20]. The Prony brake typically uses a slipping collar of radius r to exert a frictional force opposing the rotation of the output shaft. A weight W is placed on one end of a cord and a load sensor measures the force F through the other side of the cord. When the motor is switched on, the collar must overcome the friction between the cord and pulley by exerting a torque on the pulley. Starter motor torque may be found from the imbalance between W and F by summing moments about the shaft,

$$T_s = r \left(W - F \right) \tag{2}$$

The starter motor was removed from the motorcycle and assembled into the Prony brake. A pulley was fixed to the output shaft of the motor, with a cord drawn over the top of the pulley. A series of weights were hung from a loop at one end of the cord and the opposite end was attached to a load cell that was fixed to the ground. A shunt resistor was configured to measure high current draw with a voltmeter. The battery was fully charged for each test. A linear curve of the form in Eq. (1) was fit to the current-torque measurements as shown in Fig. 4. The regression constants are k_t=0.0978 N-mm/amp and I_0=18.9 amp.

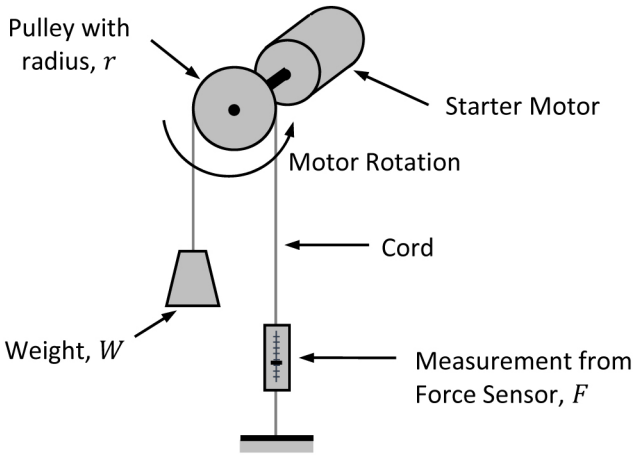

Figure 3. Prony brake test used to characterize starter motor.

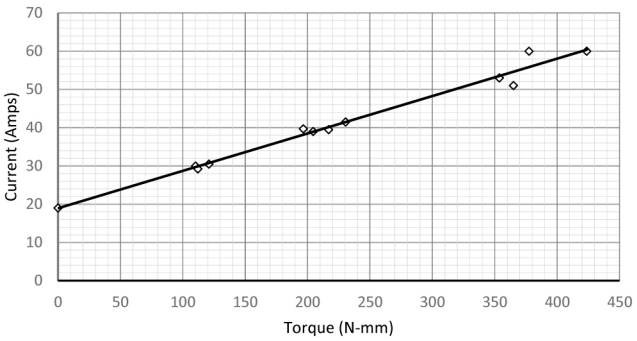

Figure 4. Relationship between starter motor torque and current draw.

Engine Starting Requirements

To characterize the starting requirements, a mean-value engine model [21] was adopted as

$$J\,\ddot{\theta}_c + T_p + T_f + T_T = R_v\,T_s, \tag{3}$$

where: J is the effective polar mass moment of inertia of the engine; $\ddot{\theta}_c$ is the acceleration of the engine shaft; T_f is the torque to overcome friction; T_p is torque required to overcome pressure buildup in the cylinder; T_T is the torque to draw in and expel gases from the engine (referred to as throttle torque); and R_v is the starter to crankshaft velocity ratio. As identified in the previous section, the test engine has R_v =27.

With the torque constant of the starter motor known, the torque transmitted by the starter motor was determined by measuring current draw during a starting cycle. The starter motor and battery were reinstalled to the motorcycle, with the shunt resistor used in earlier testing connected in series between the battery and starter motor. The voltage differential across the shunt resistor was collected with a computer data acquisition system, configured with a sampling rate of 10 kHz. The voltage signal was converted to current and ultimately starter motor torque T_s could be obtained from Eq. (1).

It was also necessary to collect data representing the engine crankshaft angle θ_c over time. A proximity sensor was configured to sense the tabs on the timing plate of the test engine and routed to a second channel on the DAQ. The test setup is shown in Fig. 5. Two test configurations were conducted to determine the engine parameters in Eq. (3). In both cases, the starter motor powered the engine, but the ignition wires were removed, preventing the engine from starting. In Configuration 1 (C-1), the spark plugs were removed, vastly reducing the pressure buildup within the cylinder. Configuration 2 (C-2) had spark plugs installed and in a standard operational mode. For testing, the ignition switch was then moved to the “on” position and the starter button pressed, cranking the engine.

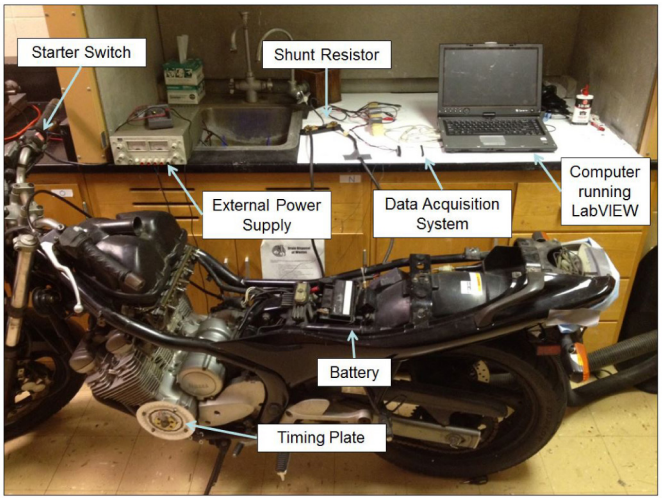

Figure 5. Engine characterization test setup.

The starter motor was kept engaged for several seconds and data was acquired. The battery was recharged in between acquisition of each data set to ensure that the energy source was constant throughout testing. A trickle charger was used, which recharges the battery with relatively low amperage, as would be the case during normal engine operation. All testing was performed indoors at approximately 21 °C. The crankshaft displacement measured by the proximity pickup during a C-2 starting event is shown as the black points shown in Fig. 6. A regression model was desired to fit the position data, so that continuous curves could be evaluated instead of finite data. An acceptable fit for the 2nd derivative of the numerical data was found to be of the form

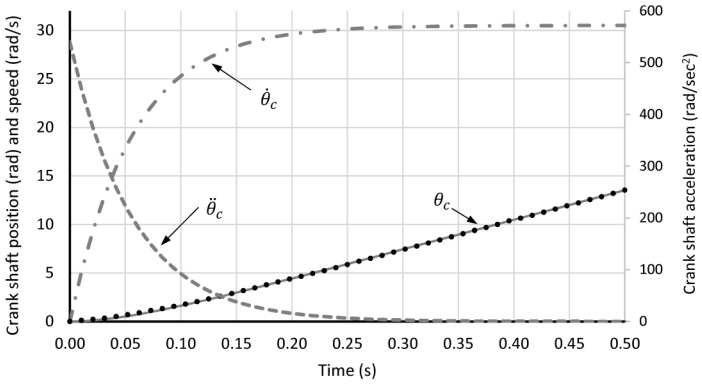

Figure 6. Crank shaft motion produced by the starter motor.

$$\ddot{\theta}_c = Ae^{Bt}. \tag{4}$$

This expression was integrated to give

$$\dot{\theta}_c = \frac{A}{B}e^{Bt} - \frac{A}{B} \tag{5}$$

where the constant of integration $C = A/B$ was determined by assigning the initial condition of $\dot{\theta}_c = 0$ when $t = 0$ and solving. Equation (5) was then integrated to give an expression for θ_c as

$$\theta_c = \frac{A}{B^2}e^{Bt} - \frac{A}{B}t - \frac{A}{B^2} \tag{6}$$

where the constant of integration was again solved for by assigning an initial condition of $\theta_c = 0$ when $t = 0$. Applying a regression algorithm to the proximity sensor data provided A = 540 rad/sec^2 and $B = -17.7$ sec^{-1}. These coefficients were substitued into Eqs. (4), (5), and (6), and plotted in Fig. 6.

Turning attention to the torque data, a representative plot from a C-1 start is shown in Fig. 7. The friction torque T_f can be obtained from C-1 test as the steady torque after the engine has achieved a constant speed. The steady- state friction is indicated in Fig. 7, noting that the measured torque at the starter is $1/R_v$ = 1/27th the torque on the crankshaft due to tha 1:27 starter transmission. The effective inertia J can be obtained from C-1 while the crankshaft is accelerating,

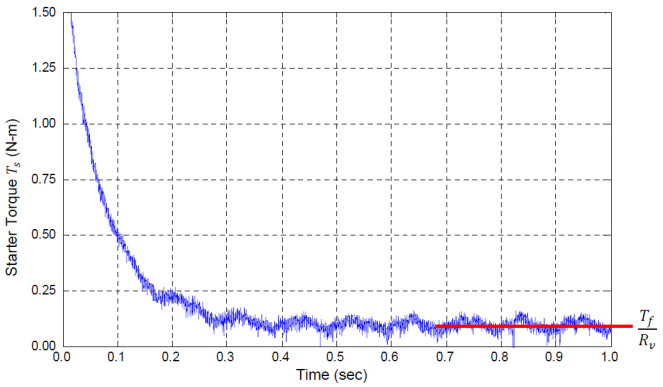

Figure 7. Torque produced by the starter motor with engine in C-1.

$$J = \frac{1}{\Delta t_s}\sum_{0}^{\Delta t_s}\frac{R_v\,T_s - T_f}{\ddot{\theta}_c}\Delta t, \tag{7}$$

where Δt_s is the duration of engine acceleration. Again, note that because of the 27:1 starter transmission, the starter torque is multiplied by R_v =27 in the numerator of Eq. (7). Applying Eqs. (7) and (4) to torque-time data from several C-1 starts, J = 0.0904 kg-m^2 and T_f = 2.56 N-m are found to adequately characterize the Yamaha XJ600S engine.

A representative plot from a start event when the engine is in C-2 is shown in Fig. 8, where the frictional torque T_f obtained from C-1 testing is labeled. The torque to overcome pressure in the cylinders T_p is observed as the peak-to-peak amplitude of the oscillating torque as noted in Fig. 8. With J, T_f, and T_p determined, Eq. 3 is used to determine the throttling torque T_T.

After several C-2 starts, T_p= 8.84 N-m, and T_T = 3.36 N-m are determined to adequately characterize the Yamaha XJ600S engine.

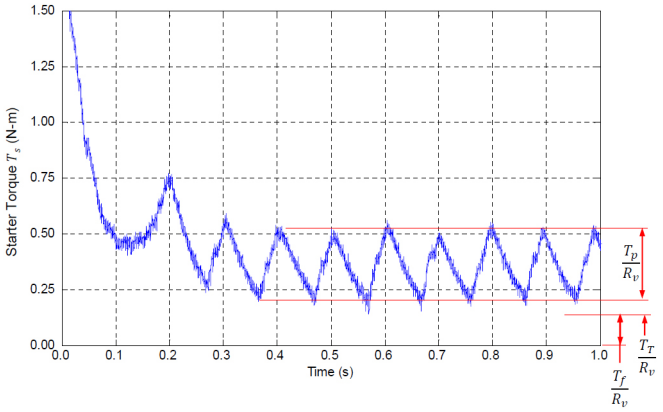

Figure 8. Torque produced by the starter motor with engine in C-2.

5. SIZING A SPRING

A schematic of a spring starter is shown in Fig. 9. It is a physical representation of Fig. 1 where energy is transferred from a wound torsional spring to the crankshaft through a transmission represented by a pair of rollers.

Engine Motion from Spring Energy

The starter spring angular displacement, velocity and acceleration is designated as θ_s, $\dot{\theta}_s$ and $\ddot{\theta}_s$, respectively. A torsional spring constant $k\theta$ relates the displacement to the torque on the spring shaft

$$T_s = k_\theta \theta_s \tag{8}$$

As before, a transmission velocity ratio between the starter and crankshaft R_v is defined such that the relationship between the starter motion and the motion of the crank is

$$\theta_c = \frac{1}{R_v}\theta_s, \qquad \dot{\theta}_c = \frac{1}{R_v}\dot{\theta}_s, \qquad \ddot{\theta}_c = \frac{1}{R_v}\ddot{\theta}_s. \tag{9}$$

The relationship between torque at the crank shaft T_c and the torque on the starter shaft is

$$T_c = R_v\,T_s. \tag{10}$$

Substituting Eq. (8) into Eq. (10),

$$T_c = R_v\,(k_\theta\,\theta_s) \tag{11}$$

Further substituting Eq. (9) into Eq. (11), gives an expression for the torque on the crankshaft due to the spring in terms of crankshaft displacement.

$$T_c = R_v^2\, k_\theta\, \theta_c$$

(12)

The rotational equation of motion for the crankshaft driven by a spring is

$$J\,\ddot{\theta}_c - R_v^2\, k_\theta\, \theta_c = -\left(T_f + T_T + T_p\right).$$

(13)

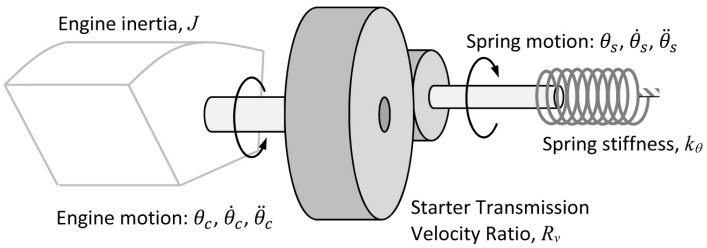

Figure 9. Schematic of spring starter.

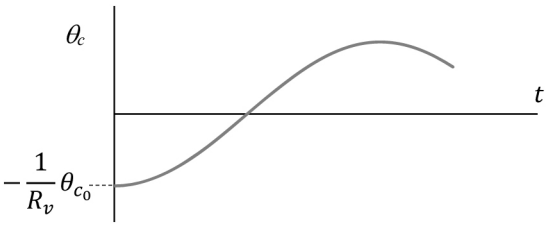

(a). Angular displacement response

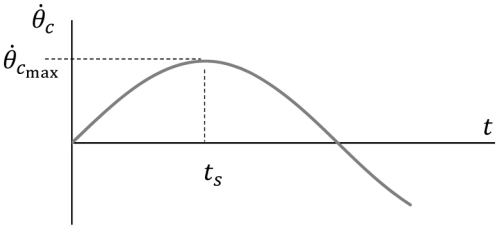

(b). Angular velocity response

Figure 10. Dynamic response of crank shaft to spring energy release.

Being a single degree-of-freedom dynamic system, the crank shaft response to releasing the spring with initial wind θ_{so} is shown in Fig. 10. The solution to the classic problem of Eq. (13) is [22]

$$\theta_c = A\cos(\omega\, t + \phi) + \frac{T_f + T_T + T_p}{R_v^2\, k_\theta},$$

(14)

where the system natural frequency is

$$\omega = \sqrt{\frac{\text{Stiffness}}{\text{Inertia}}} = \sqrt{\frac{R_v^2\, k_\theta}{J}}.$$

(15)

Reviewing Fig. 10, it is observed that $\phi = \pi$. Substituting $\theta_c = -\theta_{so}/R_v$ at $t = 0$ into Eq. (14),

$$A = \frac{\theta_{s_0}}{R_v} - \frac{T_f + T_T + T_p}{R_v^2\, k_\theta}$$

(16)

Taking the time derivative of Eq. (14),

$$\dot{\theta}_c = A\,\omega\sin(\omega\, t + \pi).$$

(17)

The crankshaft will reach its top speed $\dot{\theta}_{c_{\max}}$ at a starting time t_s. It is observed from Eq. (17) that $\dot{\theta}_c$ is maximum when $\omega t_s = \pi/2$. Thus,

$$t_s = \frac{\pi}{2}\sqrt{\frac{J}{R_v^2 k_\theta}}.$$

(18)

Also from Eq. (17), the maximum crankshaft speed obtained by the spring is

$$\dot{\theta}_{c_{\max}} = A\omega.$$

(19)

Substituting Eq. (15) into Eq. (19),

$$\dot{\theta}_{c_{\max}} = \left(\frac{\theta_{c_0}}{R_v} - \frac{T_f + T_p + T_T}{R_v^2\, k_\theta}\right)\sqrt{\frac{R_v^2\, k_\theta}{J}}.$$

(20)

Experimental values determined in the previous section were J = 0.0904 kg-m^2, T_f = 2.56 N-m, T_p= 8.84 N-m, and T_T = 3.36 N-m. Also, the steady state crankshaft speed obtained by the starter motor is $\dot{\theta}_{c_{\max}}$=30 rad/sec. The acceleration time of t_s=0.3 sec was determined. However, an engine will start once a threshold crank speed has been reached and is not dependent on the time period to reach that speed [6]. Thus, a specific value of t_s is not considered a starter requirement.

Torsional Spring Equations

For the feasibility study, a torsional steel spring was selected because of its widespread use for storing energy (specifically in garage doors) and their ability to safely dissipate energy if failure occurs. For a torsional spring, the spring constant is [23]

$$k_\theta = \frac{d^4 E}{64 D N_a}$$

(21)

where d is the spring wire diameter, E is the modulus of elasticity of the spring material, D is the mean coil diameter, and N_a is the number of active coils. The maximum bending stress in the spring wire is

$$\sigma = K_i 32T/(\pi\, d^3) \tag{22}$$

where K_i is a stress concentration factor,

$$K_i = (4C^2 - C - 1)/4C(C-1) \tag{23}$$

and $C = D/d$ is the spring index.

Optimal Spring Design

The starter design parameters include the start time t_s, gear ratio between spring and engine R_u, mean coil diameter D, wire diameter d, number of coils, N, and initial spring wind θ_{so}. Because of its established material behavior, a steel spring is selected, having a density ρ= 7.85 g/cm^3 and E=206 GPa. To avoid fatigue failure, the bending stress will be limited to the endurance strength of a medium strength spring steel, $\sigma \le 830$ MPa [17]. For feasible manufacturing, a spring index $C \ge 5$ is desired [17].

The design task involves selecting appropriate t_s, R_u, d, D, N, and θ_{so} to start the engine with the smallest possible spring. The spring size was defined by its mass

$$m_s = \frac{\rho L \pi}{4}\left[(D+d)^2 - (D-d)^2\right]. \tag{24}$$

An optimization process was conducted with the obective of minimizing m_s, subject to obtaining the crankshaft speed of $\dot{\theta}_{c_{\max}}$=30 rad/sec , limiting the spring stress to $\sigma \le 830$ MPa, and reducing manufacturing costs with C ≥5. The design parameters are related through Eqs. (20), (18), (21), (22), (23).

The optimization resulted in R_u = 1, indicating that the spring should be connected directly to the crankshaft. The objective of minimizing mass resulted in m_s = 2.3 kg. The spring had a mean coil diameter of D = 56.8 mm, a wire diameter d = 7 mm, and N = 33 coils. An initial wind of θ_{so} = 1.5 revolutions is required to start the engine. The peak torque to produce full wind is 244.0 N-m, and the time required to achieve the desired speed to start the vehicle is t_s = 0.25 sec.

6. PROTOTYPE

A proof-of-concept prototype was developed to demonstrate the viability of the design. The CAD model of a bench top mechanical starter is shown in Fig. 11 and the constructed prototype is shown in Fig. 12. For ease of demonstration, a suitable off-the-shelf garage door spring is substituted for the optimal spring identified in the previous section. The acquired spring had D = 54.4 mm, d = 5.2 mm, and N =82 coils. Substituting these values into Eq. (21), k_θ = 0.4287 N-m/rad. By applying a torque and measuring angular displacement, the spring was experimentally evaluated to verify its calculated stiffness. A discshaped weight was used in place of an engine and sized with similar equivalent inertia, calculated as J = 0.1400 kg-m^2. A drag force can be applied to the rim of the weight to simulate engine friction.

One end of the spring is coupled to a worm gear drive. Since the worm gear set is unable to back-drive, any energy stored in the spring will be retained. The other end is coupled to an output shaft via a pair of spur gears. A latching mechanism is placed between the spring and spur gears and is engaged when necessary to prevent the system from releasing energy. An overrunning clutch is mounted to the output shaft such that the system is coupled to the engine during the starting cycle and decoupled during normal engine operation. The device is charged by manually rotating the input shaft to the worm gear drive while the latching mechanism is engaged. The energy required to charge the spring may be provided by a small DC motor powered by the alternator due to the large gear reduction between the input shaft and the spring. The device is discharged by releasing the latching mechanism, thus allowing the spring to exert torque on the spur gears. The spur gears are chosen to illustrate the ease of moving the power from one shaft to another. An initial wind of 4 revolutions was supplied to the spring. No frictional force was applied. As the latch was released, the angle of the weight representing the crank shaft was measured and shown as triangular markers in Fig. 13. Substituting the appropriate values for this proof-of-concept prototype (J = 0.1400 kg-m^2, k_θ = 0.4287 N-m/rad, $T_f = T_p = T_T$ = 0) into to Eq. (14) gives the predicted response shown as the dashed curve in Fig. 13. A second test was run with a frictional torque of T_f =2.6 N-m where the results are shown as circular markers in Fig. 13 and predicted response shown with a solid curve. As is observed from the figure, the prototype operated as predicted and was considered to be successful in validating the design equations.

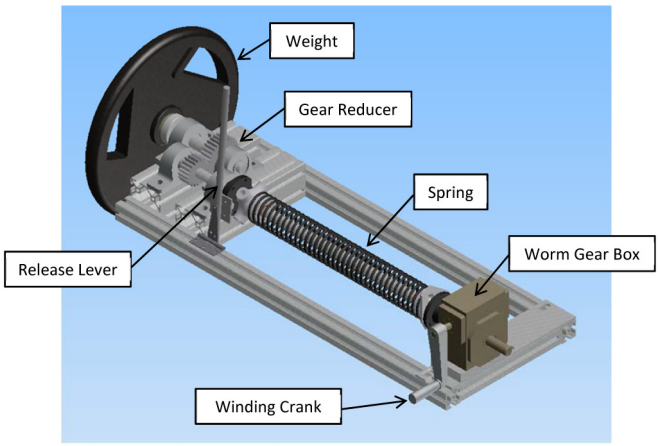

Figure 11. Model of a spring starter concept.

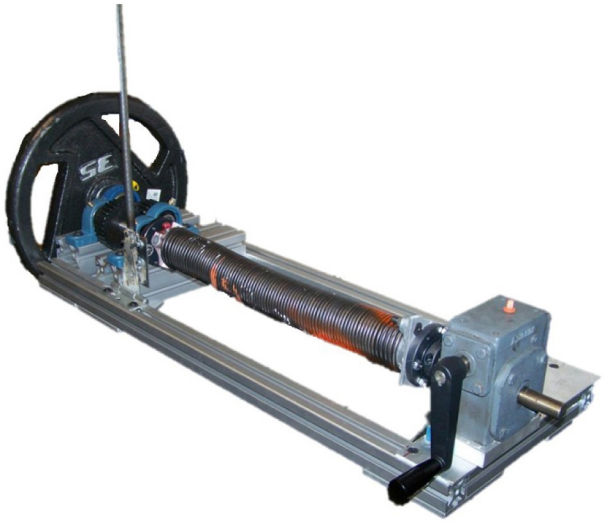

Figure 12. The spring starter concept prototype.

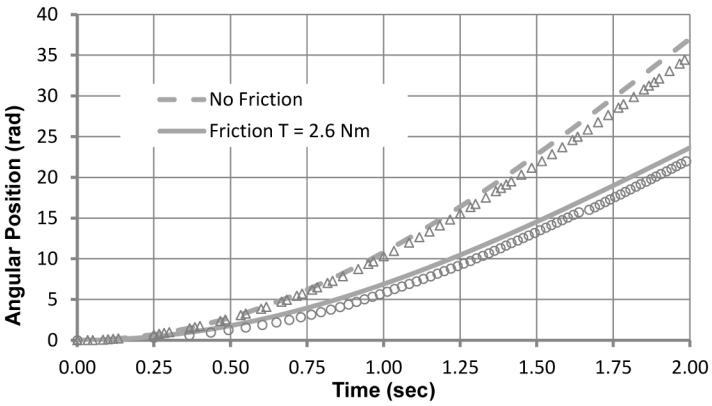

Figure 13. Proof-of-concept prototype response to an initial wind of four revolutions.

7. CONTINUED WORK

A fundamental simplification in the proof-of-concept prototype was the substitution of a disc-shaped weight in place of an engine. Additionally, an off-the-shelf garage door spring was used. For the purpose of functional testing and to determine that the system is adaptable, a second prototype is being designed to meet the starting specifications of the representative engine discussed throughout this paper (Yamaha XJ600S). The engine has been disassembled and the crankshaft is being modified to accept a direct drive start from a spring. A custom spring, with dimensions consistent with the optimization results, is being produced. Once assembled, the performance will be evaluated. Package design and reliability issues will also be assessed.

CONCLUSIONS

This paper presented the development of a optimal spring that is capable of replacing an electrical starting system for automotive application. A 600 cc, inline 4-cylinder internal combustion engine was selected to demonstrate viability. Testing was conducted to characterize the starter motor and the engine. Governing equations were arranged into an optimization, to identify a spring that is capable of starting the engine at a minimal weight. A proof-of-concept prototype has been constructed and evaluated to confirm the governing equations. Work is continuing by modifying the engine to accept the spring starting system.

REFERENCES

1. Ventura, M. J., Toh, C., Parra, C., Kremer, G. (2013) “A Study of Sustainability Adoption Trends in the Transportation Market”, *Advances in Information and Communication Technology*, 415, pp. 576-583.
2. Abedin, M.J., Masjuki, H. H., Kalam, M. A., Sanjid, A., Ashrafur Rahman, S. M., Masum B. M., (2013) “Energy balance of internal combustion engines using alternative fuels”, *Renewable and Sustainable Energy Reviews*, 26 (10), pp. 2033
3. Ettefaghi, E., Ahmadi, H., Rashidi, A., Mohtasebi, S. (2013) “Investigation of the Anti-Wear Properties of Nano Additives on Sliding Bearings of Internal Combustion Engines” *International Journal of Precision Engineering and Manufacturing*, 14(5), pp. 805-809.
4. Manning, N., Al-Ghrairi, Vermillion, S. (2013) “Designing a Hydraulic Continously Variable-Transmission (CVT) for Retrofitting a Rear-Wheel Drive Automobile”, *Journal of Mechanical Design*, 135(12), 121003.
5. Van Basshuysen, R. and Schaefer, F., “Internal Combustion Engine Handbook,” Society of Automotive Engineers, Inc., Warrendale, PA, ISBN 978-0-7680-11395, 2004, doi:10.4271/R-345.
6. Bosch, R. (2004)*Bosch Automotive Handbook*, 8/e, Wiley Publishing Company, Hoboken, New Jersey.
7. Ingram, A. (2012) “The Electric Self-Starter Turns 100”, *High Gear Media*, Feb. 15.
8. Kettering, C. (1915) *Engine Starting Device*, U.S. Patent No. 1,150,523.
9. Linden, T. (2010)*Handbook of Batteries*, 4/e., McGraw-Hill, New York.
10. Bishop, J., Nedungadi, A., Ostrowski, G., Surampudi, B.et al., “An Engine Start/Stop System for Improved Fuel Economy,” SAE Technical Paper 2007-01-1777, 2007, doi:10.4271/2007-01-1777.
11. McManus, M. C. (2012). “Environmental Consequences of the Use of Batteries in Low Carbon Systems: The Impact of Battery Production”, *Applied Energy*, 93(5), pp. 288-295.
12. Ashby, M.F. (2011) *Materials Selection in Mechanical Design*, 4/e, Elsevier Ltd., Oxford, U.K.
13. Hill, F. A., Havel, T., Livermore, C. (2009). “Modeling Mechanical Energy Storage In Springs Based On Carbon Nanotubes”, *Nanotechnology*, 29.
14. Briggs & Stratton Corporation (2011) *Operating and Matenenance Instructions for IntekE and Quantumr with Touch-N-Mowr Starter*.
15. Startwell Engineering (2013) “Startwell Mechanical Starters”, http://www.startwell.com.
16. Hoppie, L.O. (1982). “The Use of Elastomers in Regenerative Braking Systems”, Rubber Chemistry and Technology: March 1982, 55(1), pp. 219-232.
17. Carlson, H. (1995) Spring Designer's Handbook, 2/e.
18. Ahlstrand, A., Haynes, J. H. *Yamaha XJ600S & XJ600N Service and Repair Manual, Haynes, Somerset*, England, 2004.
19. Alciatore, D. G., Histand, M. B. (2007) *Introduction to Mechatronics and Measurement Systems*, 3/e, McGraw-Hill, New York.
20. Gindy, S. S. (1985). “Force and Torque Measurement, A Technology Overview Part II Torque”, *Experimental Techniques*, 9(7), pp. 9-14.
21. Guzzella, L., Onder, C. *Introduction to Modeling and Control of Internal Combustion Engine Systems*, Springer, 2010.
22. Rao, S. (2011) *Mechanical Vibrations*, 5/e, Prentice-Hall, Upper Saddle River, NJ.
23. Shigley, J., Mischke, C., Budynas, R. (2004) *Mechanical Engineering Design*, 7/e, McGraw-Hill Publishing Company, New York.